

# Plane Polarization of 15.1-Mev Bremsstrahlung from 25-Mev Electrons\*

D. JAMNIK† AND P. AXEL

*Physics Department, University of Illinois, Urbana, Illinois*

(Received July 20, 1959)

Linearly polarized gamma rays were produced with the aid of a special betatron doughnut which made it possible to limit the effective thickness of the bremsstrahlung-producing Al and Pt targets. The linear polarization of 15.1-Mev bremsstrahlung gamma rays was detected by measuring the azimuthal angular distribution of gamma rays which had been scattered elastically from the well-known nuclear level in  $C^{12}$ .

For the particular effective thickness of Al that was used, the maximum polarization of 15.1-Mev gamma rays in the bremsstrahlung of 25-Mev electrons was  $1.53 \pm 0.05$ . (This corresponds to 21% in the more conventional polarization notation.) Both this observed maximum (which occurred at an angle of  $1.4^\circ$ ) and the polarization measured at four other angles confirm theoretical predictions.

With the platinum target that was used, the observed polarization of  $1.28 \pm 0.04$  was about 10% lower than the value predicted by theoretical calculations which use the Born approximation and neglect screening. However, available screening and Coulomb corrections bring the theoretical predictions into essential agreement with the experimental values.

Since the elastic scattering pattern of gamma rays shows unambiguously that the strong photon scattering level at 15.1 Mev in  $C^{12}$  is excited by magnetic dipole radiation, this level has spin 1 and even parity.

## I. INTRODUCTION

THE experimental work on polarized bremsstrahlung reported in this paper differs from previous work in three respects:

1. A modified betatron doughnut was constructed which made it possible to limit the effective target thickness in a reproducible way. The effective thickness of a 10.5-mg/cm<sup>2</sup> Al target was limited to 30 mg/cm<sup>2</sup> while the 5.4-mg/cm<sup>2</sup> Pt target was limited to 10.5 mg/cm<sup>2</sup> despite electron beam divergence or recirculation.

2. The elastic scattering of gamma rays was used to detect the polarization of medium energy gamma rays (i.e., 15 Mev). This polarization detection technique has the advantage of giving low background effects while producing statistically significant data in a relatively short time.

3. Linearly polarized gamma rays produced by an electron accelerator were used to learn about a property (i.e., the parity) of a nuclear energy level.

The original purpose of this experiment was to find the degree of linear polarization that could be attained in bremsstrahlung produced by a betatron. After polarization had been detected, the experiment was extended to check the reliability of the approximate calculations then available. Recent improved theoretical calculations remove most of the discrepancy between the theory and the experimental results. However, even the best theoretical treatment available contains approximations which discourage the tedious auxiliary calculations needed before the experiments can be used as a very precise check of the theory.

In a bremsstrahlung process, the production plane is defined as the plane which contains the lines of motion

of the incident electron and the emerging gamma ray. Partial linear (or plane) polarization implies that the intensity of gamma radiation whose electric vector is perpendicular to the production plane,  $I_\perp$ , is different from the intensity whose electric vector is in the production plane,  $I_\parallel$ .

The conventional definition of the polarization,  $\pi$ , is

$$\pi \equiv (I_\perp - I_\parallel) / (I_\perp + I_\parallel). \quad (1)$$

It will be more convenient, in this paper, to use the alternate definition of the polarization:

$$P \equiv I_\perp / I_\parallel = (1 + \pi) / (1 - \pi). \quad (2)$$

$P$  is a function of the incident electron energy,  $E_e$ , the emitted photon energy,  $E_\gamma$ , and the angle between them,  $\theta$ . For  $E_e \gg mc^2$  (where  $m$  is the electron mass),  $I_\perp > I_\parallel$  except in a very small energy region near the maximum value of  $E_\gamma$ ; hence, as  $P$  is defined in Eq. (2),  $P > 1$ . As a function of  $E_\gamma$ ,  $P$  increases as  $E_\gamma$  decreases. As a function of  $\theta$ ,  $P = 1$  for  $\theta = 0$  or for  $\theta \gg mc^2/E_e$ ;  $P$  has a maximum value at about  $\theta = mc^2/E_e$ . Because of the dependence of  $P$  on  $\theta$ , the maximum polarization can be attained only if a perfectly collimated electron beam strikes an infinitely thin bremsstrahlung target. In most experiments, beam divergence and multiple electron scattering in the target before bremsstrahlung reduce the achievable polarization.

In this experiment,  $P$  was determined by comparing the intensity of photons scattered perpendicular to the production plane,  $N_\perp$ , to the intensity of photons scattered in the production plane,  $N_\parallel$ . If the scattering were a pure electric dipole process  $I_\perp$  could contribute only to  $N_\parallel$  but not to  $N_\perp$ . (This corresponds to the classical fact that an oscillating charge does not radiate in the direction of its acceleration.) Similarly,  $I_\parallel$  would contribute to  $N_\perp$  but not to  $N_\parallel$ . For a magnetic dipole scattering process, on the other hand,  $I_\perp$  contributes only to  $N_\perp$  while  $I_\parallel$  contributes to  $N_\parallel$ . Since it is known

\* Supported in part by the joint program of the Office of Naval Research and the U. S. Atomic Energy Commission.

† Visitor from J. Stefan Institute, Ljubljana, Yugoslavia.

from theory that  $I_1 > I_{11}$ , if one finds  $N_1 > N_{11}$  for a dipole scattering, this scattering must be magnetic dipole. In this case (and for the experiment described below),

$$P = N_1/N_{11} \quad (\text{magnetic dipole}); \quad P > 1. \quad (3)$$

In order to restrict the scattering to either magnetic dipole or electric dipole, it was particularly convenient to use the scattering from a single nuclear energy level. The 15.1-Mev level in  $C^{12}$  is ideal for this purpose because it overwhelmingly dominates the scattering of high-energy gamma rays by carbon.<sup>1</sup> For 15.1-Mev gamma rays produced by 25-Mev electrons impinging on an infinitely thin Al bremsstrahlung target, theory predicts a polarization of  $P = 1.83$  for  $\theta = \theta_0 = mc^2/E_e = 0.02$  radian. For a 30-mg/cm<sup>2</sup> aluminum target,  $P$  is reduced to about 1.35 at  $\theta = \theta_0$  and has a maximum value of about  $P = 1.47$  at  $\theta = 1.6\theta_0$ .

Section II summarizes earlier experiments. The available calculations are reviewed in Sec. III. The arrangement used in this experiment is discussed in Sec. IV which includes measurements of the angular distribution of the bremsstrahlung; this angular distribution is used as a measure of the effective target thickness. The polarization measurements are given in Sec. V, and comparison between theory and experiment is given in Sec. VI.

## II. EARLIER EXPERIMENTS

The features of the theory of bremsstrahlung polarization were verified in experiments with 1-Mev electrons performed by Motz.<sup>2</sup> His results indicate some limitations in the theoretical calculations that had been made in this low-energy region, but it is not clear what this discrepancy implies about the validity of the theoretical approximations used at about 20 Mev.

Although four experiments have been done in the energy range from 11.5 Mev to 25 Mev, the results cannot be compared easily, and only one of the experiments can be compared with theory. In all of these experiments, photographic emulsions were used to detect the angular distribution of photoprotons from deuterium. This technique, which had been used effectively by Wilkinson<sup>3</sup> to study complete polarization, has limited applicability in the study of partial polarization because of poor statistics and background effects.

The first three measurements could not be interpreted easily because the bremsstrahlung were produced by an internal target in either a betatron or a synchrotron. The effective target thickness was uncertain due to the possible existence of edge effects in the target, of electron beam divergences, and of electron beam recircula-

TABLE I. Values of polarization given by Dudley, Inman, and Kenney.

Angle of observation	Earlier results <sup>a</sup>		Later results <sup>b</sup>	
	$\pi = \frac{(P-1)}{(P+1)}$	Tracks	$\pi$	Tracks
$\theta_0 = mc^2/E_e$	$0.242 \pm 0.081$	396	$0.242 \pm 0.181$	396
$1.6\theta_0$	$0.157 \pm 0.095$	260	$0.38 \pm 0.15$	600
$2.5\theta_0$	$0.123 \pm 0.102$	255		

<sup>a</sup> See reference 7.

<sup>b</sup> See reference 8.

tion. In none of these measurements were data given on the bremsstrahlung angular distribution (from which the effective target thickness might be inferred). Phillips<sup>4</sup> used a betatron to produce a 20-Mev bremsstrahlung spectrum from a 5-mil wolfram target. Despite poor statistics (a total of 500 tracks were measured in four different areas of unspecified position), Phillips concluded that photoprotons were produced preferentially at both 90° and 20°. Muirhead and Mather<sup>5</sup> used a synchrotron to produce 11.5-Mev bremsstrahlung from a 5-mil platinum target. When they grouped their 1165 proton tracks into three groups corresponding to different gamma-ray energies, they found anisotropy only in the 180 tracks arising from gamma rays between 7.5 Mev and 11.5 Mev. Since the polarization should be higher for the lower energy gamma rays, Muirhead and Mather doubted that they had a polarized bremsstrahlung beam. Tzara<sup>6</sup> used a betatron to produce 22-Mev bremsstrahlung from a 0.8-mil target. Using 438 photoproton tracks from 0.2 cm<sup>2</sup> of D<sub>2</sub>O-loaded emulsion, and 110 background tracks from 0.168 cm<sup>2</sup> of an H<sub>2</sub>O-loaded emulsion, Tzara reported a surprisingly high polarization,  $P = 3.5 \pm 0.5$ .

Dudley, Inman, and Kenney<sup>7</sup> avoided the ambiguities of a circular accelerator by using 25-Mev electrons from a linear accelerator to produce a bremsstrahlung spectrum in a 1-mil Al target. The photoprotons from deuterium, detected in D<sub>2</sub>O-loaded emulsions, came mainly from 4-Mev to 8-Mev gamma rays. The results as originally reported<sup>7</sup> and those corrected for larger background effects (which were found later<sup>8</sup>) are summarized in Table I. Although the data clearly show polarization effects, they are not sufficiently precise to test the theory.

## III. AVAILABLE CALCULATIONS

### A. Bremsstrahlung

The existence of polarization in nonrelativistic bremsstrahlen was pointed out by Sommerfeld.<sup>9</sup> A theoretical treatment for the relativistic case was first given by

<sup>4</sup> K. Phillips, Phil. Mag. **44**, 169 (1953).

<sup>5</sup> E. G. Muirhead and K. B. Mather, Australian J. Phys. **7**, 527 (1954).

<sup>6</sup> C. Tzara, Compt. rend. **239**, 44 (1954).

<sup>7</sup> Dudley, Inman, and Kenney, Phys. Rev. **102**, 925 (1956).

<sup>8</sup> Verbal report by R. W. Kenney to Conference on Photonic Reactions, National Bureau of Standards, April 30, 1958 (unpublished).

<sup>9</sup> A. Sommerfeld, Ann. Physik **11**, 257 (1931).

<sup>1</sup> Fuller, Hayward, and Svantesson, Bull. Am. Phys. Soc. **1**, 21 (1956); E. Hayward and E. G. Fuller, Physica **22**, 1138 (1956); E. Hayward and E. G. Fuller, Phys. Rev. **106**, 991 (1957).

<sup>2</sup> J. W. Motz, Phys. Rev. **104**, 557 (1956).

<sup>3</sup> D. H. Wilkinson, Phil. Mag. **43**, 659 (1952).

May and Wick<sup>10</sup> who used the method of virtual quanta<sup>11</sup> together with the polarization dependence of the Compton effect to find the expected bremsstrahlung polarization. Subsequently, May<sup>12</sup> calculated the polarization more accurately using the Born approximation ( $Z \ll 137$ ) for the electron wave functions. Before summing over the directions of the emergent electrons May specialized his results to the case of complete screening. (This corresponds to the approximation  $E_e \gg 137Z^{-1}mc^2$ ; or  $E_e \gg 30$  Mev for Al, and  $E_e \gg 16$  Mev for Pt. This is analogous to the treatment given by Bethe<sup>13</sup> for bremsstrahlung summed over polarization.) Gluckstern, Hull, and Breit<sup>14,15</sup> derived the same differential formula.<sup>15</sup> This was summed over the emergent electrons by Gluckstern and Hull<sup>16</sup> (to give a formula analogous to the well-known unscreened Bethe-Heitler formula<sup>17</sup>). Gluckstern and Hull also made a crude screening correction which is applicable at very low gamma-ray energies. The effect of screening was treated more accurately by Fronsda and Überall<sup>18</sup> who used the Born approximation together with an exponential form factor to account for screening. (This treatment of screening had been used by Schiff<sup>19</sup> in the bremsstrahlung calculations summed over polarization.) Finally, Olsen and Maximon<sup>20</sup> included both a Coulomb correction and a screening correction based on the Thomas-Fermi potential. (This more accurate treatment of screening corresponds to the Bethe-Heitler screening correction.<sup>17,21</sup>) These corrections bring the bremsstrahlung polarization calculations to the same advanced stage that was reached earlier for pair production and integrated bremsstrahlung calculations.<sup>22-26</sup> However, even these calculations involve approximations which neglect terms of the order of  $mc^2/(E_e - E_\gamma)$  which in our case is 0.05.

For the theoretical polarization and angular distribution of bremsstrahlung from Al we used the values

<sup>10</sup> M. May and G. C. Wick, *Phys. Rev.* **81**, 628 (1951).

<sup>11</sup> C. F. von Weizsäcker, *Z. Physik* **88**, 612 (1934); E. J. Williams, *Kgl. Danske Videnskab. Selskab, Mat.-fys. Medd.* **13**, No. 4 (1935).

<sup>12</sup> M. M. May, *Phys. Rev.* **84**, 265 (1951).

<sup>13</sup> H. A. Bethe, *Proc. Cambridge Phil. Soc.* **30**, 524 (1934).

<sup>14</sup> Gluckstern, Hull, and Breit, *Science* **114**, 480 (1951).

<sup>15</sup> Gluckstern, Hull, and Breit, *Phys. Rev.* **90**, 1026 (1953).

<sup>16</sup> R. L. Gluckstern and M. M. Hull, Jr., *Phys. Rev.* **90**, 1030 (1953).

<sup>17</sup> H. A. Bethe and W. Heitler, *Proc. Roy. Soc. (London)* **A146**, 83 (1934).

<sup>18</sup> C. Fronsda and H. Überall, *Phys. Rev.* **111**, 580 (1958).

<sup>19</sup> L. I. Schiff, *Phys. Rev.* **83**, 252 (1951).

<sup>20</sup> H. Olsen and L. C. Maximon, *Phys. Rev.* **114**, 887 (1959); and private communication.

<sup>21</sup> H. A. Bethe and Julius Ashkin, in *Experimental Nuclear Physics*, edited by E. Segrè (John Wiley and Sons, Inc., New York, 1953), Vol. 1.

<sup>22</sup> Bethe, Maximon, and Low, *Phys. Rev.* **91**, 417 (1953).

<sup>23</sup> H. A. Bethe and L. C. Maximon, *Phys. Rev.* **93**, 768 (1954).

<sup>24</sup> Davies, Bethe, and Maximon, *Phys. Rev.* **93**, 788 (1954).

<sup>25</sup> Haakon Olsen, *Phys. Rev.* **99**, 1335 (1955).

<sup>26</sup> Olsen, Maximon, and Wergeland, *Phys. Rev.* **106**, 27 (1957); Olsen, Wergeland, and Maximon, *Bull. Am. Phys. Soc.* **3**, 174 (1958).

given by Fronsda and Überall.<sup>27</sup> This seemed most suitable inasmuch as the Coulomb correction is negligible and the entire screening correction is about the same size as the error introduced for  $Z=0$  by neglecting terms of order  $mc^2/(E_e - E_\gamma)$ . (This is true for 15-Mev bremsstrahlung from 25-Mev electrons in an Al target where the screening correction is only about 2%; for 5-Mev bremsstrahlung, however, screening reduces the maximum polarization by more than 25%.) Since the entire screening correction is small, there seemed little point in being concerned about whether the Fermi-Thomas potential or the exponential form of the atomic potential was used. On the other hand, for the Pt target both the screening correction and the Coulomb correction are appreciable. Therefore, the theoretical values for the polarization and angular distribution of bremsstrahlung were taken from Olsen and Maximon.<sup>20</sup> [It is known that the neglect of  $mc^2/(E_e - E_\gamma)$  predicts too low a polarization by about 3% for  $Z=0$  at  $\theta = mc^2/E_e$ , but no estimate is available of the error in polarization or angular distribution at finite  $Z$ .]

The theoretical polarizations used are shown as a function of angle in Fig. 1 together with the values<sup>16</sup> for  $Z=0$ ; the values are for  $E_e=25$  Mev and  $E_\gamma=15$  Mev. The corresponding theoretical angular distributions of the intensity are shown in Fig. 2. The values for aluminum give a slightly broader angular distribution than is given by the unscreened Bethe-Heitler formula. The values for platinum give a still broader distribution which, however, agrees very well with the formula,  $N(\theta) = [1 + (\theta/\theta_0)^2]^{-2}$ ; this is the usual approximation<sup>28</sup> to the angular distributions calculated by Schiff.<sup>19</sup>

## B. Effects of Electron Beam Angular Divergence

Because the polarization varies strongly with angle any angular spread in the electrons which produce bremsstrahlung will affect the experimentally observed angular dependence of polarization. If the exact electron angular distribution were known, it could be used together with the theoretical angular dependence of the total bremsstrahlung intensity to obtain the appropriate average of the intrinsic angular dependence of polarization.

Although the angular divergence of the electron beam is not known if this beam strikes an internal target in a circular electron accelerator, the resulting angular distribution of the total bremsstrahlung intensity might be a reliable guide to the initial electron divergence. One way to proceed with the interpretation of data would be to use several reasonable guesses of the electron beam divergence and to use the measured angular

<sup>27</sup> Obtained from the IBM-704 computer in Paris using the CERN-2 program devised by Fronsda and Überall; see reference 18.

<sup>28</sup> L. H. Lanzl and A. O. Hanson, *Phys. Rev.* **83**, 959 (1951).

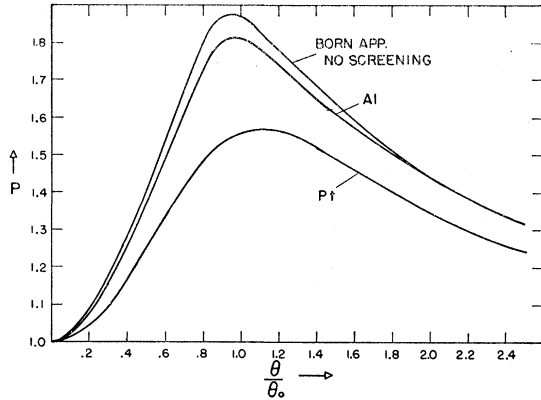


FIG. 1. Theoretical polarization of 15-Mev bremsstrahlung from 25-Mev electrons. The target is assumed to be infinitely thin. The top curve is for  $Z=0$ ; it is taken from reference 34 and is based on the formulas in reference 16. The middle curve which is for aluminum ( $Z=13$ ) is based on references 18 and 27. The bottom curve applies to platinum ( $Z=78$ ) and is based on reference 20.

distribution of the total bremsstrahlung intensity to select the most suitable electron distribution. Since the calculation of the expected bremsstrahlung distribution is quite tedious, we used as a sample electron distribution one which would be appropriate for an initially collimated electron beam after it had been multiply scattered in the bremsstrahlung target. For our purposes it is not important to know whether this electron distribution takes multiple scattering into account very accurately inasmuch as only our experimental bremsstrahlung results can justify the use of any electron distribution. (Fortunately, as will be shown in Sec. IV, our results agreed well enough with these calculations to make calculations with other electron distributions unnecessary.) However, because an accurate treatment of multiple scattering may be useful in other experiments, we shall comment below on the accuracy of the electron distribution we use if it is applied to experiments involving collimated electron beams and targets of finite thickness.

A good approximation for the distribution of electrons which radiate after having been scattered through angles,  $\theta$  and  $\varphi$ , into a solid angle,  $d\Omega$ , is given by

$$N(\theta, \varphi, m_t) d\Omega = \frac{1}{2\pi m_t^2 \theta_0^2} [-Ei(-\theta^2/2m_t^2 \theta_0^2)] d\Omega; \quad (4)$$

$\theta_0 = mc^2/E_e$ ,  $m_t$  is a constant which depends on both the target material and the total thickness  $t$ , and

$$[-Ei(-x)] = \int_x^\infty \frac{e^{-y}}{y} dy,$$

the exponential integral function. (Note that  $m$  is the electron mass but  $m_t$  and  $m_r$  are parameters depending on target thickness.) Equation (4) would be appropriate if two conditions were satisfied. First, as indicated by

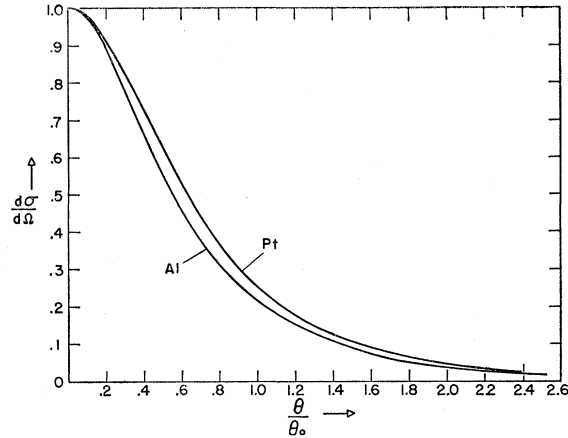


FIG. 2. Angular distribution of bremsstrahlung intensity. The curves show the angular distribution of the 15-Mev gamma rays resulting when 25-Mev electrons strike an infinitely thin target. The narrower angular distribution applies to aluminum; it is taken from the data of references 18 and 27. Complete neglect of screening as in reference 16 would give a slightly narrower distribution. The broader angular distribution which applies to platinum is based on reference 20.

the approximate calculation of Williams,<sup>29</sup> electrons which have been multiply scattered by a foil of thickness,  $\tau$ , should emerge with a Gaussian angular distribution given by

$$f(\theta, \varphi, \tau) d\Omega = \frac{1}{2\pi m_r^2 \theta_0^2} \exp[-(\theta^2/2m_r^2 \theta_0^2)] d\Omega. \quad (5)$$

Incidentally, Eq. (5) shows the physical interpretation of  $m_r$ ; it is the ratio of the root mean square scattering angle to  $1.41\theta_0$ :

$$m_r = [\langle \theta_s^2 \rangle_{AV}]^{1/2} / 1.41\theta_0. \quad (6)$$

The second condition needed for deriving Eq. (4) is that  $m_r$  be proportional to the square root of the thickness<sup>29</sup>:

$$m_r^2 \propto \tau. \quad (7)$$

When a bremsstrahlung target of thickness,  $t$ , is used, electrons will have been multiply scattered because of having traversed various thicknesses,  $\tau$ , before producing bremsstrahlung. It is therefore necessary to sum the expression given in Eq. (5) over the thickness range,  $0 \leq \tau \leq t$ . If Eq. (7) were correct, this sum would be given by  $N(\theta, \varphi, t)$  as in Eq. (4).

An improved calculation of multiple electron scattering by Molière,<sup>30</sup> and by Bethe,<sup>31</sup> was confirmed experimentally by Hanson, Lanzl, Lyman, and Scott.<sup>32</sup> Hanson *et al.* also showed that this more accurate theory can be approximated by a Gaussian, and the convenient formula which they give<sup>32,31,33</sup> matches the

<sup>29</sup> E. J. Williams, Phys. Rev. **58**, 292 (1940).

<sup>30</sup> G. Molière, Z. Naturforsch. **3a**, 78 (1948).

<sup>31</sup> H. A. Bethe, Phys. Rev. **89**, 1256 (1953).

<sup>32</sup> Hanson, Lanzl, Lyman, and Scott, Phys. Rev. **84**, 634 (1951).

<sup>33</sup> D. R. Corson and A. O. Hanson, *Annual Review of Nuclear Science* (Annual Reviews, Inc., Palo Alto, 1953), Vol. 3, p. 67.

accurate theory to within 1% for the target thicknesses important in this polarization experiment. Thus, the Gaussian electron distribution [Eq. (5)] is accurate but the dependence of  $m_r$  on  $\tau$  is not that given in Eq. (7).

Since Eq. (7) is not correct, the accurate value of  $N(\theta, \varphi, m_i)$  can be obtained only from numerical integration. In order to find the error introduced by using Eq. (4) for  $N$ , an accurate numerical integration was carried out to find the angular distribution of bremsstrahlung producing electrons in a 25-mg/cm<sup>2</sup> Al target. The resulting electron angular distribution was very similar to that given by Eq. (4) except that a value of  $m_i=0.54$  had to be used in Eq. (4) whereas the true value of  $m_i$  for 25 mg/cm<sup>2</sup> is  $m_i=0.56$ . Thus, using Eq. (4) for the electron angular distribution would not introduce any appreciable error if the value of the parameter,  $m_i$  is properly reinterpreted.

For the present experiment the reinterpretation of  $m_i$  in terms of thickness is unimportant because  $m_i$  can be treated as a parameter which is inferred from measurements of the angular distribution of bremsstrahlung and which is then used to calculate the expected angular distribution of polarization. Because of this, Eq. (4) was used for the electron distribution. [In the remainder of this paper, when a target thickness is inferred from an  $m_i$  value, it will be adjusted upward by 8% in an attempt to remove the error introduced by using Eq. (4). This adjustment is made even though the uncertainty about the actual electron distribution and the errors involved in measuring  $m_i$  exceed this small correction.]

After the electron distribution of Eq. (4) was accepted, it was necessary to calculate the angular dependence both of the total bremsstrahlung intensity and of the polarization for various values of the parameter,  $m_i$ . Some of the necessary calculations had already been done by Miller<sup>34</sup> who used the intrinsic bremsstrahlung angular distribution and polarization given by Gluckstern and Hull.<sup>16</sup> These calculations, which were all that were available while the measurements were being made, were an extremely useful guide to the experimental work. When the improved theoretical approximations became available<sup>18,20,27</sup> we made the more exact calculations necessary to interpret our results.

Because Miller's calculations did not include the effect of screening, they underestimate the angular spread of the intrinsic bremsstrahlung intensity. A simple way to supplement Miller's calculations involves following the procedure of Lanzl and Hanson<sup>28</sup> who use a two-Gaussian approximation to the simple form they suggest for the intrinsic "Schiff spectrum." This procedure gave angular distributions somewhat different from those of Miller but at least part of the discrepancy is due to the approximations made by Lanzl and

Hanson. Our final calculations were done more exactly with the aid of the Illiac, a digital computer at the University of Illinois. For the platinum target the angular distributions were almost identical with those of Miller except that the value of  $m_i$  implied by a given distribution was less by 0.1. For the aluminum target the exact angular distributions were somewhat different. If the measure of  $m_i$  was taken as the full width of the experimental angular distribution at the  $\frac{1}{2}$  maximum or  $\frac{1}{4}$  maximum points, the actual  $m_i$  values were less than those predicted by Miller by 0.07 or 0.03, respectively. Although the measured angular distributions could not be obtained with enough precision to distinguish clearly between Miller's calculations and our more accurate values, the experimental data were in somewhat better agreement with the more accurate values. (Other calculations of the effect of target thickness on the angular distribution<sup>35</sup> are not particularly appropriate to this work because they deal with considerably thicker targets.) It should be emphasized that uncertainties in  $m_i$  are not very important if one wants to check the polarization calculations semiquantitatively inasmuch as a shift in  $m_i$  by 0.05 usually changes the expected polarization by less than 2%.

#### IV. EXPERIMENTAL ARRANGEMENT AND THE ANGULAR DISTRIBUTION OF BREMSSTRAHLUNG

If a betatron is used conventionally, the linear polarization of bremsstrahlung is probably obscured because of the angular divergence of the electron beam before the gamma rays are produced. Usually, the main cause of this beam divergence is the multiple scattering of electrons in the (normally thick) target. Even if an especially thin bremsstrahlung target is used, electrons which pass through the target without radiating can recirculate through the betatron and strike the target several additional times,<sup>36</sup> thereby producing an effectively thick target. A second cause of electron beam divergence may be radial oscillations of the electron beam, particularly as it is moved from the stable orbit to the target. Precautions which were taken to eliminate beam recirculation and excessive radial oscillations are described below.

##### A. Special Doughnut Including Beam Stopper

In order to reduce beam recirculation the special doughnut shown in Fig. 3 was used in the Illinois 25-Mev betatron.<sup>37</sup> A 60-mil piece of wolfram (2.9 g/cm<sup>2</sup>) which was placed 163° from the target acted as a beam stopper to intercept electrons which had been scattered in the target. The precise effect of the beam stopper

<sup>35</sup> A. Penfold, thesis, University of Illinois, 1955 (unpublished); A. S. Penfold and J. E. Leiss, University of Illinois Report, May, 1958 (unpublished); A. Sirlin, Phys. Rev. **101**, 1219 (1956); **106**, 637 (1957). E. Hisdal, Phys. Rev. **105**, 1821 (1957); Arch. Math. Naturvidenskab **54**, No. 3, 1 (1957).

<sup>36</sup> Fuller, Hayward, and Koch, Phys. Rev. **109**, 630 (1958).

<sup>37</sup> D. W. Kerst, Rev. Sci. Instr. **13**, 387 (1942).

<sup>34</sup> J. Miller, privately circulated report, C.E.A. No. 655, Centre d'Études Nucléaires de Saclay, 1957 (unpublished).

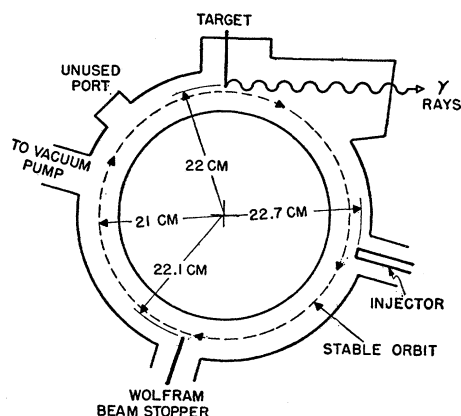


FIG. 3. Special betatron doughnut. The thick wolfram beam stopper ( $2.9 \text{ g/cm}^2$ ) is  $163^\circ$  away from the thin bremsstrahlung target. The radial distances shown are those used in the polarization experiments. For other measurements, the positions of the stable orbit, the target, and the stopper were varied.

depends on how the magnetic field,  $H$ , varies with the radius,  $r$ , at the position of the target. This variation is given by the field index,  $n$ , which is defined as  $n = (-r/H)(\partial H/\partial r)$ .

If  $n$  were known, the stopper action could be predicted by using the convenient formula given by McMillan,<sup>38</sup> which takes into account the effects of both scattering and energy loss in the target. For example, for 25-Mev electrons, a  $10.5\text{-mg/cm}^2$  target of aluminum, and a field index of  $n = \frac{3}{4}$ , McMillan's formula predicts that the energy loss would reduce the radial position of the beam by 0.7 mm near the target and by 0.35 mm near the stopper (about  $180^\circ$  away). Scattering in the target would not affect the radial shift,  $\Delta r$ , near the scatterer. For scattering,  $\Delta r \propto \sin[(1-n)^{1/2}\theta]$  (where  $\theta = 0$  at the target position), and there would be a radial shift near the stopper; this shift would be alternately positive and negative on successive circulations of the beam. Because of this and because the stopper has a much larger area, the electrons which are scattered excessively at the target should hit the stopper before they can hit the target a second time.

Under normal conditions, the Illinois betatron operates with a value of  $n = \frac{3}{4}$  at the stable orbit.<sup>37</sup> However, in this experiment the value of  $n$  was uncertain both because the radial position of the target was somewhat larger than usual and because the expansion pulse might affect  $n$ . The target and stopper configuration shown in Fig. 3 should have provided effective stopping if the field index was near  $n = \frac{3}{4}$ . Both the target and the stopper could be moved in all three dimensions.

Stoppers of several different shapes were tried; some of them had notches near where the electron beam would hit. The notches did not seem to affect the angular distribution in the horizontal plane but they did improve the vertical angular distribution slightly. The stopper which was used for the polarization run

was a 1.7-cm square which had a small semicircular notch of 2-mm radius. The vertical position of the stopper was adjusted so that the notch was centered about the plane in which the electrons moved. The target was placed in this same plane.

The stopper effectiveness was tested at a number of different target radii; at each target radius a number of different stopper positions were tried. The bremsstrahlung angular distribution seemed to depend only on the relative radial positions of the target and the stopper. These studies of the dependence of the angular distribution on the radial position of the stopper were made to see whether there were gross changes in the stopper action. There was little reason for studying this systematically with high precision because it was very desirable to keep the relative radial distance between the injector and the stopper as small as possible. When the stopper moves radially inward it attenuates the circulating electron beam at injection.

## B. Orbit Expansion

In the Illinois betatron the electron beam is forced to spiral radially outward from the stable orbit to the target.<sup>37</sup> This orbit expansion is produced by supplying a pulse of current to expander coils which produce more accelerating flux and less magnetic field than would be appropriate for the stable orbit. (Since the expander pulse does affect the magnetic field between the stable orbit and the detector, it might affect the field index,  $n$ .) If a very rapid expander pulse were used, appreciable radial oscillations of the electron beam might result. A rapid expander pulse would also have the disadvantage of producing a short duration pulse of electrons, thereby complicating the electronic detection of scattered gamma rays.

In order to avoid these difficulties, the expander pulse was made relatively slow.<sup>39</sup> A gradual expansion was used which required about 200 microseconds for the beam to move radially the 1 cm from the stable orbit to the target. During this time the electrons traveled  $6 \times 10^6 \text{ cm}$ , making about  $4.4 \times 10^4$  revolutions; this implies a spiral path whose average pitch is about  $2.2 \times 10^{-5} \text{ cm}$ . This spiral pitch is consistent with the fact that with a beam diameter of about 1 mm, the electrons continued to hit the target for about a 20-microsecond time interval during each of the 180 pulses per second. (Both "pinhole camera" pictures and collimators were used to locate and to measure the size of the region where the electron beam hit the target.)

## C. Effective Target Thickness

The effective thickness of the target was determined by measuring the angular distribution of bremsstrahlung and by comparing the full angular width at both  $\frac{1}{2}$  and  $\frac{1}{4}$  maximum with the calculated values. Two

<sup>38</sup> E. M. McMillan, Rev. Sci. Instr. **22**, 117 (1951).

<sup>39</sup> T. J. Keegan, Rev. Sci. Instr. **24**, 472 (1953).

different techniques were used for measuring the angular distributions and both gave the same results. The first method consisted of measuring the  $(\gamma, n)$  radioactivity induced in long copper strips which were irradiated 1 meter from the target. An end window Geiger counter with a small collimating hole was used to examine the copper strip at  $\frac{1}{4}$  inch intervals. (These intervals corresponded to angular intervals of about 0.0063 radian or  $0.36^\circ$ ; the angle  $\theta_0 = mc^2/E_e$  was 0.0204 radian or  $1.17^\circ$ .) Using this system, a measurement of the vertical and horizontal angular distribution required about 25 minutes (including irradiation time).

The second technique, which was designed to reduce the measuring time, used a small cylindrical ionization chamber whose diameter was  $\frac{1}{4}$  inch. This cylinder was mounted 1 meter from the target with its axis parallel to the incident electron beam; the entire chamber was moved both horizontally and vertically by remote control. An auxiliary beam monitor was used to guarantee the constancy of the betatron yield.

Figure 4 shows the angular distributions obtained for three different relative radial positions of the target and the beam stopper. The experimental data can be brought into excellent agreement with the calculated curves by adjusting the parameter  $m_t$  in the theoretical curve and by subtracting a small known isotropic component from the experimental points. Since many other sets of experimental data were also consistent with calculated angular distributions, it seemed reasonable to use these data together with the calculations to define the effective value of  $m_t$  (the target thickness). (It was necessary to show experimentally that the angular distributions were similar to those calculated since there is no simple way to predict that the effective electron angular divergence before bremsstrahlung in a

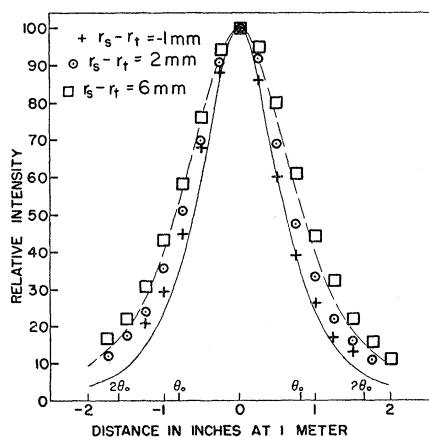


FIG. 4. Angular distribution for several target and stopper positions. The graph shows the relative intensity (normalized to 100 at the maximum) as a function of the distance from the beam center. The three series of experimental points can be fitted by curves similar to the two theoretical curves shown if the parameter  $m_t$  is varied. The solid theoretical curve corresponds to  $m_t = 0.5$  while  $m_t = 1.0$  for the dashed curve; both of these curves neglect screening.

betatron will be the same as that in a target which is actually thick.)

The effect, on both the  $m_t$  value and the yield, of varying the radial position of the target for a fixed stopper position is shown in Fig. 5. The yield was measured with the narrow ( $\frac{1}{4}$ -in. diameter) ionization chamber which subtended  $0.36^\circ$  in the center of the beam when it was 1 meter from the target. This ionization chamber was calibrated at 20 r/min at 1 meter against a Victoreen Ionization Thimble enclosed in an 8-cm Lucite cube. Since the yield was measured in the forward direction and since the beam has a greater angular spread for larger stopper to target separations, the total yield increases more rapidly than is shown by the points in Fig. 5.

The angular distributions summarized in Fig. 5 had full widths at  $\frac{1}{4}$  maximum which varied from 0.050 to 0.072 radian; a pure intrinsic Schiff spectrum would have given a width of  $2mc^2/E_e$  or 0.040 radian. The

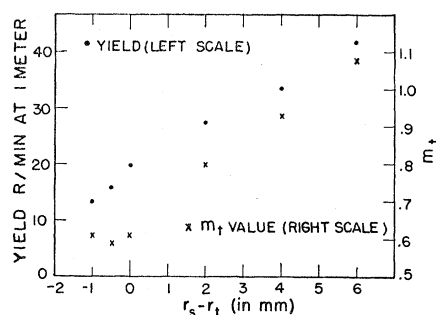


FIG. 5. Effect of relative positions of target and stopper on yield and on effective thickness. The dots and the left scale show the yield in forward direction. The crosses and the right scale show the  $m_t$  values as inferred from the angular distribution with screening neglected. The abscissa is the radial difference between stopper and target positions. The radius of the inner edge of the target is  $r_t$ ; that of the stopper is  $r_s$ . (The notch in the stopper corresponds to a radius 2 mm greater than  $r_s$ .)

corresponding effective thicknesses are 30 mg/cm<sup>2</sup> and 91 mg/cm<sup>2</sup> of Al; the actual thickness was 10.5 mg/cm<sup>2</sup>.

The experimental data of Fig. 5 were used to choose a target and stopper geometry for the polarization tests. The inner edge of the target was set at a radius which was a fraction of a millimeter above that of the inner edge of the stopper so that the target extended slightly into the notch in the stopper. This positioning was checked indirectly from time to time by measuring the angular distribution; no changes equivalent to shifts in  $m_t$  greater than 0.05 were ever found.

The data of Fig. 5 do not provide detailed information about the recirculation of the beam and the effectiveness of the stopper. The increase in the yield as the target was moved radially inward with respect to the stopper showed clearly that there is beam recirculation if the stopper is not effective. (Auxiliary experiments had shown that the target positions did not affect the beam which circulated in the stable orbit. Furthermore, the

expansion pulse was always large enough to deliver essentially the entire electron beam to radii as large as that of the stopper.) However, it is not possible to match the data of Fig. 5 quantitatively by assuming simple beam trajectories and perfect stopper action. For example, it is clear that the angular distribution does not continue to improve (i.e.,  $m_t$  does not continue to decrease) as the target is moved radially outward into the stopper notch. Since the minimum  $m_t$  value obtainable with a 10.5-mg/cm<sup>2</sup> Al target corresponded to a thickness of 30 mg/cm<sup>2</sup>, some effect was causing a divergent electron beam to strike the target. One possible explanation is that some electrons were scattered from the edge of the stopper. (It is also possible that unknown peculiarities of the field index,  $n$ , at the time of expansion caused divergence or allowed recirculation. However, this possibility seems unlikely since the angular distributions were surprisingly insensitive to expander pulse shape as well as to the radial position of the target-stopper pair.)

Bremsstrahlung angular distribution measurements were also made in the plane perpendicular to the electron orbit. This vertical distribution was very slightly broader than the horizontal distributions discussed above. The  $m_t$  values calculated from the vertical distributions were about 0.03 larger than those calculated from the horizontal distributions. This difference is not at all surprising since both the stopper actions and the electron beam oscillations are different for vertical and horizontal deflections.

#### D. Final Angular Distribution Measurements

The polarization studies were made for a single effective target thickness of aluminum and a slightly greater effective thickness of platinum. Figure 6 shows the bremsstrahlung angular distribution in the horizontal plane for each target; Fig. 6(a) is for aluminum whereas Fig. 6(b) is for platinum. The aluminum data indicate  $m_t=0.57$  while the platinum data correspond to  $m_t=0.64$ . These  $m_t$  values correspond to effective thicknesses of about 30 mg/cm<sup>2</sup> for the actual 10.5-mg/cm<sup>2</sup> Al target and 10.5 mg/cm<sup>2</sup> for the actual 5.4-mg/cm<sup>2</sup> Pt target.

These bremsstrahlung angular distributions were checked before, during, and after each of the polarization runs. In addition, angular distributions were measured for the different tangential positions of the target which were used to vary the angular position of the gamma-ray beam in order to allow different portions of the beam through the collimator. The variations in  $m_t$  never exceeded 0.05; this maximum variation in  $m_t$  was not far from the limit of the experimental precision. (It would correspond to an error of about 1/20 inch or 2.5% in the full width of the angular distribution pattern at one-quarter intensity as measured at 1 meter. Such variation could also be produced by making an error of 8% in the monitor reading or 2%

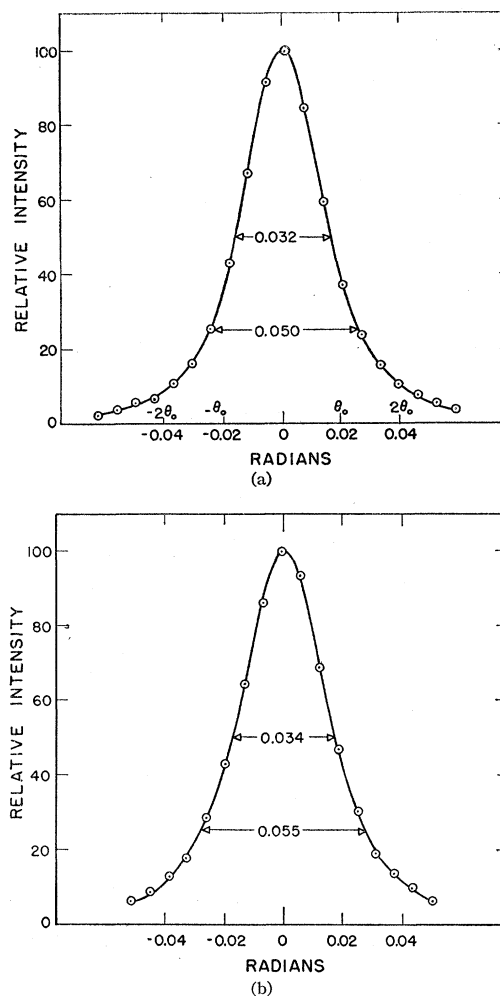


Fig. 6. Bremsstrahlung angular distributions from polarization targets. Figure 6(a) shows the angular distributions for Al; the  $m_t$  values inferred from this curve is 0.57. The data for platinum in Fig. 6(b) imply  $m_t=0.64$ . The full widths, in units of radians are given at 1/2 and 1/4 maximum.

in the reading of the small ionization chamber.)<sup>1</sup> An error in  $m_t$  of 0.05 would produce a maximum error in the value of  $P$  of about 2.6%; however, for most angles the shift in  $P$  caused by a shift of 0.05 in  $m_t$  is closer to 1%.

### V. POLARIZATION MEASUREMENTS

#### A. Experimental Procedure

The polarization of 15.1-Mev gamma rays was measured by detecting the azimuthal angular distribution of gamma rays elastically scattered from C<sup>12</sup>. A scale drawing of the geometry of the experimental arrangement is shown in Fig. 7. The defining aperture of the main 2-foot thick iron collimator was about 45 inches from the bremsstrahlung target; the full angular spread of the collimated beam was 0.50° or 0.43θ<sub>0</sub> at the electron energy of 25 Mev (kinetic energy of electron



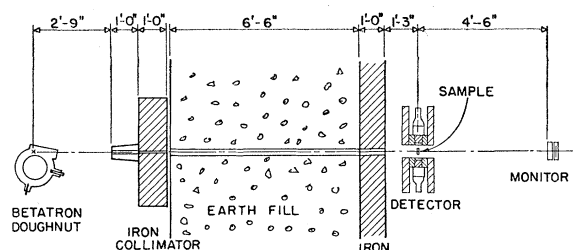


FIG. 7. Scale drawing of polarization experiment geometry.

24.5 Mev). The beam passed through a brass pipe inserted in the 6-foot thick earth fill which made up the rear wall of the betatron building; an auxiliary one foot thick iron shield was set beyond this wall. The carbon scattering sample was about 14 feet from the bremsstrahlung target; at this position the beam diameter was about 1.5 inches. A thick-walled ionization chamber placed 4.5 feet beyond the sample served as a beam monitor.

The carbon scattering sample was made of polystyrene; its thickness was  $1.93 \text{ g/cm}^2$ . The front face of the 5-in. diameter, 4-in. thick NaI crystal detector was 6.7 in. from where the center of the beam hit the sample. The effective crystal diameter was reduced to 3.5 in. by means of 4-in. thick Pb shielding. The finite solid angle subtended by the detector introduced a correction of from 0 to 2% in the polarization. In order to attenuate preferentially low-energy gamma rays and thereby avoid pulse pileup, a composite absorber of 2.75-in. graphite and about  $\frac{1}{4}$ -in. Pb was used in front of the crystal throughout the experiment. (In some runs in series I, the Pb absorber thickness was increased when the beam intensity on the sample increased; during series II, the betatron yield reaching the sample was maintained constant despite shifts in angle, and a  $\frac{3}{8}$ -in. Pb absorber was used for all points.)

The crystal and phototube were surrounded by a cylindrical Pb shield with walls that were 3 in. thick. The entire scintillation setup, including the shielding, was mounted on a wheel which made it possible to change the azimuthal angle while keeping the radial distance constant to within  $\frac{1}{2}\%$ . In series II, two detectors  $180^\circ$  apart were used.

The electronic system used to record the scattered gamma rays was completely conventional. A 7046 photomultiplier (14 dynode) was operated at about 2500 volts with a 180-ohm load resistor. The pulses from the phototube were transmitted directly over 180-ohm cable to a remote counting area. They were then amplified with a linear feedback amplifier, and sent through a simple diode clipper and stretcher to a 100-channel pulse-height analyzer. The gain and clipping were such that the analyzer recorded pulses above about 5 Mev and each channel accepted pulses in a 250-keV energy interval.

The entire experimental procedure was designed to eliminate errors which might result from slow shifts in

either gain or monitor sensitivity. The data were collected in individual runs which were only about 10 minutes long. Between runs the detector was rotated through  $90^\circ$  and a radioactive source ( $\text{Na}^{22}$ ) was observed; a constant attenuator was used so that the standard 511-keV gamma-ray photopeak and the 15.1-Mev scattered gamma-ray produced equal output pulses from the amplifier. Each time the phototube was rotated through  $90^\circ$ , a gain shift of about 10% was introduced to compensate for the effect of the earth's magnetic field on the phototube gain. Between 8 and 24 runs were added together to give a single value of the polarization at a given angle.

The angular portion of the beam transmitted through the collimator was changed by shifting the angle between the center of the main beam and the axis of the collimator (i.e., the line between the center of the collimator and the bremsstrahlung target). The angle could be changed easily by shifting the tangential position of the target with respect to the electron orbit. The shifted beam position was located photographically at about 1 meter from the target. The beam which was about 2 cm in diameter could be located to within  $\pm \frac{1}{2}$  mm corresponding to an angular uncertainty of about  $\pm 0.03\%$  at 25 Mev. The center of the main beam was always set so that the production plane of the gamma rays going through the collimator was horizontal.

## B. Measurement of Background

Due to the finite resolution of the NaI crystal, the 15-Mev "photopeak" extends from about 12 Mev to 16 Mev. In this energy range the background at the detector is quite low and comes almost entirely from gamma rays scattered elastically and inelastically from the nuclei in the scattering sample. This background was determined in three different ways.

(1) A  $5.54\text{-g/cm}^2$  graphite absorber was placed in the collimated beam before the carbon scattering sample. The nuclear absorption of this graphite attenuated the detected 15-Mev gamma rays to about 30% of their original value; the nuclear absorption was obtained by correcting for the atomic absorption of 10% and for the monitor response. The resultant pulse spectrum, although it still had a prominent 15-Mev peak, had a small enough peak-to-background ratio to permit a reliable estimate of the background. An upper limit of 11% and a lower limit of 7% to the background were obtained from this curve. From these values, it was possible to estimate the background as 9% of the average of the vertical and horizontal counting rates.

(2) An equivalent water sample was placed in the beam instead of the standard polystyrene sample. Although the nuclear scattering from oxygen might well be different from that of carbon, one would expect a similarity except for the strong scattering 15.1-Mev level in carbon. The counting rate obtained with the water sample in place also corresponded to 9% of the

average of the vertical and horizontal counting rates when the carbon scatterer was used.

(3) The background due to inelastic scattering was estimated from the parameters found by Garwin<sup>40</sup> who studied photon scattering in carbon. Garwin gives the integrated cross sections for the elastic scattering by the 15.1-Mev level (2.33 mb Mev), and for nonresonant elastic scattering from neighboring levels (0.1 mb Mev). He also measured the contribution of gamma rays in this energy region from the inelastic scattering of higher energy gamma rays. Furthermore, Garwin gives the ratio of the Doppler width to the total level width from which one can calculate the absorption of the resonant gamma rays in the polystyrene scattering sample. Using these data, one calculates a background of 8% for this experiment. This value is in excellent agreement with the 9% value which we used in analyzing the data. (Garwin's parameters also predicted correctly the effect of the 5.54-g/cm<sup>2</sup> graphite absorber.)

It is conceivable that the background is different in the vertical and horizontal positions of the detector because of polarization. If the background came from *M1* processes, there would be more in the vertical than in the horizontal direction, whereas if it came from *E1* processes the background would be larger in the horizontal direction. Since the gamma-ray background above the 15-Mev line was symmetric we had no choice but to assume that there were no polarization effects in the background. (The measurements made with a graphite beam absorber did not have sufficient statistical accuracy to give information about whether the background in the 15-Mev region was polarized.)

### C. Polarization Data

Each polarization point was obtained by adding together the data from a set of runs. Between each run the detection system was rotated through 90° so that vertical and horizontal data were taken alternately. Furthermore, on alternate vertical runs the detector would be either above or below the sample while both the east and the west positions were obtained in the horizontal runs. (The beam ran from north to south.) During the runs of series I the main beam was east of the collimator while during series II the beam was west of the collimator. The shielding was good enough to eliminate differences in the east and west counting rates that might have been caused by faulty attenuation of the main beam. However, if the horizontal detector had always been set on only one side of the beam, a small (1%) correction would have been necessary to account for the nonuniform bremsstrahlung intensity across the target. (If the edge of the target nearest the detector received the larger intensity, the effective detection efficiency would be slightly larger in the horizontal position.)

<sup>40</sup> E. L. Garwin, Phys. Rev. **114**, 143 (1959).

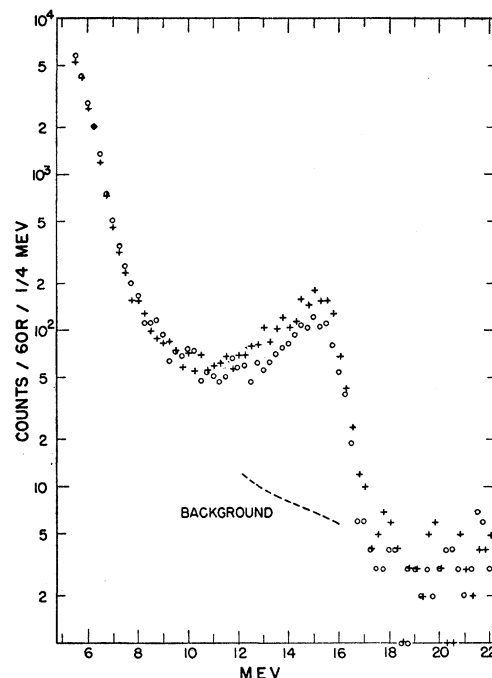


FIG. 8. Energy spectrum of scattered gamma rays. The illustrated background was measured in auxiliary experiments described in the text. The data correspond to entry 1 in Table II; the sum of 12 vertical runs is shown as crosses and 12 horizontal runs are shown as open circles.

The typical set of data (used to obtain a single polarization point) shown in Fig. 8 illustrates the pulse-height spectrum obtained. The counts in the region between 12 Mev and 16.25 Mev are mainly those from the 15-Mev gamma ray of interest. The open circles in Fig. 8 represent the sum of 12 runs with the detector horizontal. The corresponding data for 12 runs with the detector vertical are shown by the crosses. The background for 12 runs, as obtained from auxiliary measurements, is shown in Fig. 8 by the dashed line.

The counts that were used to obtain the polarization were those in the energy interval between 12.25 Mev and 16 Mev. (No attempt was made to calibrate the energy response or to adjust the energy accepted per channel of the pulse-height analyzer.) The horizontal scale of Fig. 8 and the energies quoted in this discussion are only approximate. However, using this energy scale gives a much clearer idea of the experimental procedure than would a discussion based solely on channels in the analyzer.) The particular energy interval was chosen to minimize the error that would be introduced by a slight shift in the entire energy interval. In order to test the possible influence of an energy shift, the 3.75-Mev interval was divided in each series of runs into three 1.25-Mev intervals. Ratios between these three intervals were quite sensitive to exact energy limits, and a shift of 100 kev in the relative energy scale for the vertical and horizontal data usually produced statistically significant distortions. In order to have a fixed, consistent

TABLE II. Summary of polarization data.

I Target	II Total $E$ MeV	III $E\theta/mc^2$	IV Polarization <sup>a</sup> vert. - back (hor. - back)	V Total counts vert.	VI Total counts 12.25 Mev to 16 Mev hor.	VII back	VIII Total time minutes	IX Total intensity $r$	X No. of runs	XI Scintil. absorber Pb inches	XII Resonant <sup>b</sup> counts/r vert.	XIII counts/r hor.
Series I (1 counter)												
1. Al	25	1.31	$1.57 \pm 0.07$	1552	1051	117	300	120	24	1/4	23.9	15.6
2. Al	25	1.58	$1.52 \pm 0.11$	623	433	48	180	51	16	1/4	22.5	15.1
3. Al	25	0.73	$1.24 \pm 0.09$	505	378	40	76	80	8	5/8	21.5	15.6
4. Al	25	0.0	$1.02 \pm 0.05$	900	882	80	89	160	8	5/8	19.0	18.5
5. Al	25	1.31	...		1236	111	161	60	12	1/4	18.8	
6. Al	21.2	1.31	$1.44 \pm 0.08$	897	647	54	370	70	14	1/4	24.0	16.9
7. Al	18.8	1.31	$1.17 \pm 0.08$	539	470	35	315	51	16	1/4	19.8	17.1
8. Pt	25	1.43	$1.30 \pm 0.05$	933	740	75	194	80	16	1/4	21.4	16.6
9. Pt	25	1.64	$1.30 \pm 0.07$	771	610	62	307	83	26	3/8	21.0	16.2
10. Pt	25	0.98	$1.17 \pm 0.05$	1363	1191	115	190	200	20	1/2	18.8	16.2
Series II (2 counters)												
11. Al	25	1.31	$1.49 \pm 0.06$	1780	1251	136	191	92	18	3/8	43.8	29.7
12. Al	25	1.61	$1.47 \pm 0.06$	1773	1267	137	305	92	18	3/8	43.6	30.1
13. Al	25	0.87	$1.33 \pm 0.05$	2052	1598	164	170	103	20	3/8	44.9	34.1
14. Al	25	0.36	$1.08 \pm 0.04$	1641	1531	143	138	92	18	3/8	39.9	37.0
15. Al	25	0.0	$0.97 \pm 0.04$	1358	1392	124	134	82	16	3/8	36.9	38.0
16. Pt	25	1.61	$1.27 \pm 0.05$	1424	1158	116	141	72	14	3/8	44.6	35.6

<sup>a</sup> Polarization values given are corrected for the finite solid angle of the detector as well as for background.

<sup>b</sup> The relative number of scattered 15-Mev gamma rays per roentgen on the target is corrected to the value that would have been obtained with a  $\frac{1}{4}$ -in. Pb absorber in front of NaI scintillator.

analysis procedure, we adjusted the relative energy scale in each run so that the counting rate ratios from the three 1.25-Mev channels were the same. The required shift was always small, if a shift was necessary at all. Furthermore the shift never produced a significant change in the ratio of the counts obtained in the entire 3.75-Mev interval.

A summary of the polarization data is given in Table II. Column I gives the bremsstrahlung target material, column II the total electron energy including rest mass, and column III gives the angle between the main beam and the center of the scattering sample in units of  $\theta_0$ . Column IV gives the final value of polarization corrected for background and for the finite solid angle subtended by the detector. The errors shown are statistical. Columns V, VI, and VII give the data from which the polarization was calculated. The background shown in column VII should be subtracted from both the vertical and horizontal counts shown in columns V and VI, respectively, in order to get the 15-Mev gamma-ray contribution. Columns VIII to XI indicate the experimental conditions under which the data were obtained. About  $\frac{1}{2}$  of the time shown in column VIII and exactly half of the  $r$  shown in column IX were used for the vertical runs which were one-half the value given in column X. Column XI gives the thickness of Pb absorber used in front of the scintillator. Columns XII and XIII give the number of resonant counts (with background subtracted) that would have been obtained per  $r$  if the Pb absorber in front of the scintillator had been  $\frac{1}{4}$  in. Columns XII and XIII should average about a common, nonpolarized value. In almost all cases the averaging was perfect. However, there are several entries which indicate a slight slow

shift of the monitor response. (The monitor response was not corrected for air temperature and pressure because the temperature did not fluctuate significantly during any series of runs that corresponded to a single entry in Table II.) These shifts in no way affect the calculated polarization.

The data taken from row 5 of Table II were obtained with the detector at angles midway between the vertical and horizontal positions. These data combined with those of row 1 are shown in the polar plot of Fig. 9. Since the incoming gamma ray beam is polarized with its electric vector at  $0^\circ$  and  $180^\circ$ , the pattern shows that the scattered radiation is  $M1$  (magnetic dipole). Since the  $C^{12}$  ground state is  $0+$ , the scattering state must be  $1+$ .

If the background, which was taken as 9% were as high as 11% the polarization would increase by less than 1%. If the background itself had maximum anisotropy due to polarization the inferred polarization would change by 2% or less depending on whether the background was dominated by  $E1$  or  $M1$  transitions.

## VI. COMPARISON WITH THEORY

The experimentally observed polarizations of 15.1-Mev gamma rays from 25-Mev bremsstrahlung are shown by the points in Fig. 10. The solid curves are those resulting from calculations which used the values discussed in Sec. III [i.e., the bremsstrahlung polarizations shown in Fig. 1, the bremsstrahlung angular distributions shown in Fig. 2, and the electron angular distribution of Eq. (4)]. The theoretical curves in Fig. 10 differ somewhat from those given by Miller<sup>34</sup> partly because he used the unscreened Born approximation values for bremsstrahlung, and partly because

his procedure for determining the thick-target polarization overestimates the resultant polarization.

Two minor modifications were made to the data of Table II in order to obtain the points shown in Fig. 10. First, in the four cases in which it was appropriate, the data obtained in series I were averaged with the corresponding data of series II; the lines in Table II which were combined are 1 and 11, 2 and 12, 4 and 15, and 9 and 16. The second adjustment was a slight shift in angle which was made in order to take into account the finite angular interval ( $0.43\theta_0$ ) across the scattering sample. Due to this finite angle, the expected polarization would not be that at the angle corresponding to the center of the beam but rather at some nearby angle. Rather than correct the theoretical curves for this finite angle, we chose to shift the experimental points to the angle at which the polarization should be the same as the average polarization over the actual finite angular interval. The appropriate angle was calculated by using the measured angular distribution of bremsstrahlung and the theoretical curves shown in Fig. 10. For example, the polarization observed in the angular interval from  $0.66\theta_0$  to  $1.09\theta_0$  which is centered at  $0.87\theta_0$  was plotted in Fig. 10 at  $0.84\theta_0$ . Other points were shifted by similarly small angles which varied from  $0.01\theta_0$  to  $0.04\theta_0$ .

In addition to the statistical errors which are shown in Fig. 10 there are a number of other possible sources of small errors. The uncertainty in the background would introduce an error of less than 1%; if the background were completely polarized the error might be

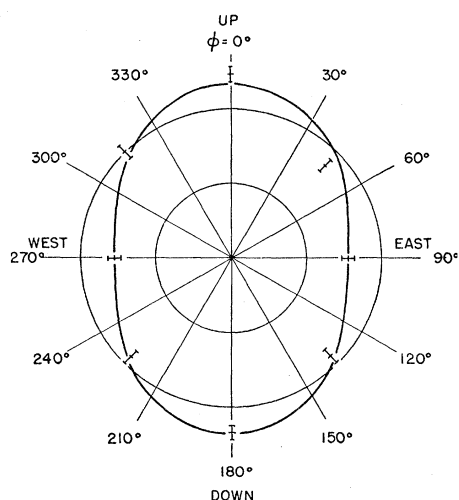


FIG. 9. Azimuthal angular distribution of elastically scattered 15-Mev gamma rays. This is a polar plot in which the radial scale is in counts per r. The inner circle corresponds to 10 counts/r; the outer circle corresponds to 20 counts/r. The average value of the 8 data points is 19.2 counts/r. Background has been subtracted and 1% detection efficiency corrections have been made to compensate for the position. The solid curve is given by: (counts/r) =  $15.4(1 + 0.51 \cos^2 \phi)$ . This corresponds to  $P = 1.53$ ; 0.51 is appropriate rather than 0.53 due to the finite solid angle of the detector.

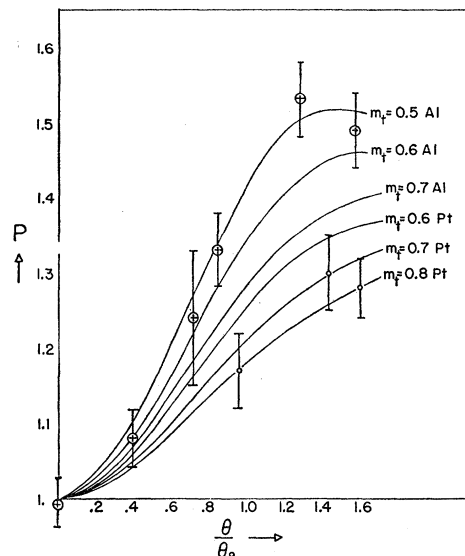


FIG. 10. Polarization as a function of angle. The experimental points shown are for 15.1-Mev bremsstrahlung gamma rays arising from 25-Mev electrons. The crosses surrounded by circles are for the Al target with  $m_t = 0.57$ ; the small circles are for Pt with  $m_t = 0.64$ . The statistical errors are shown. The solid curves are those given by the calculations discussed in the text.

2%. The angular position of the beam is uncertain to  $\pm 0.03\theta_0$ . Gain instability or channel shift could be responsible for errors of 1.5% or less. The value of  $m_t$  is probably known to 0.05; shifts of  $m_t$  during the course of the experiment of 0.03 would have gone undetected. It is impossible to put exact limits on the errors that would be introduced if the actual electron angular distribution were somewhat different from that of Eq. (4) without doing tedious, unfruitful calculations. However, not much error is involved as is indicated by the very good agreement between the experimental results and the theoretical calculations for the angular distribution of both the total bremsstrahlung intensity and the polarization. One final possible source of error is the uncertainty in the exact energy of the electron beam. This energy was determined as 25 Mev (or 24.5-Mev kinetic energy) by using a linear extrapolation of the Illinois betatron calibration. Previous experiments at Illinois have shown the betatron to be linear to 20 Mev and we could find no evidence for significant saturation or nonlinear effects. An error of 0.5 Mev in the initial electron energy would introduce an error of about 0.04 in the peak value of  $P$  for an infinitely thin aluminum target. This error would be increased slightly due to the change in expected angular distribution.

The polarization data taken with the aluminum target and shown in Fig. 10 are in excellent agreement with the theoretical curve. The  $m_t$  value deduced from the angular distribution of bremsstrahlung was  $m_t = 0.57 \pm 0.05$ . The data taken with the platinum target have polarizations only slightly below what is expected for

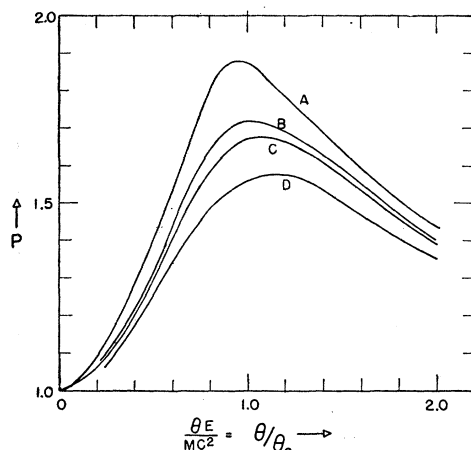


FIG. 11. Polarization from infinitely thin platinum target. The curves apply to 15-Mev gamma rays in 25-Mev bremsstrahlung. Curve *A* uses Born approximations without screening (references 16 and 34). Curve *B* is for Born approximation and exponential screening correction (references 18 and 27). Curve *C* is for Born approximation with Thomas-Fermi screening, while curve *D* includes both Thomas-Fermi screening and Coulomb correction (reference 20). Terms of order  $(mc^2/E_e - E_\gamma) = 0.05$  were neglected in calculating both curve *C* and curve *D*.

$m_t = 0.64 \pm 0.05$ . (The polarization data, in this case imply a value of about  $m_t = 0.75$ .) Although the experimental results are by no means good enough to establish any inadequacy in the theory, one possible source of this slight disagreement is the approximate nature of the theoretical calculation for platinum. Figure 11 shows the predictions of different approximations for the polarization expected from 15-Mev bremsstrahlung produced by 25-Mev electrons in a platinum target.

Curve *D* (which is also shown in Fig. 1 as the curve on which the calculations of Fig. 10 are based) is obtained by neglecting terms of order  $mc^2/(E_e - E_\gamma)$  which is 0.05. For  $Z=0$  calculations, this neglect reduces the polarization; if this approximation always tended to predict too low a polarization, the disagreement in Fig. 10 would be worse.

The data taken at 21.2 Mev and 18.8 Mev with the aluminum target (see Table II, entries 6 and 7) were not compared quantitatively with the theory. Semiquantitative checks which were made showed that the decreased polarizations were about what would be expected for 15-Mev bremsstrahlung gamma rays produced by these lower energy electrons.

If one would like to check the theory of bremsstrahlung polarization more precisely and establish the effect of neglecting  $mc^2/(E_e - E_\gamma)$ , better experiments should be performed using collimated electron beams and targets of known thickness. On the other hand, these experimental results clearly establish the validity of the theory as at least a semiquantitative and probably a quantitative guide.

#### ACKNOWLEDGMENTS

We should like to thank Professor A. O. Hanson for suggestions and stimulating discussions. We are also indebted to Mr. J. S. O'Connell who did some of the early work at Illinois on the detection of the 15-Mev gamma ray in carbon. These experiments benefitted greatly from the careful cooperation of the betatron operators under the direction of Mr. R. P. Wardin. Mr. P. M. Baum and Mr. R. S. Jones kindly coded the numerical calculations for Illiac.